



Published in final edited form as:

*Exp Neurol.* 2009 April ; 216(2): 342–356. doi:10.1016/j.expneurol.2008.12.008.

## Doublecortin expression in adult cat and primate cerebral cortex relates to immature neurons that develop into GABAergic subgroups

Yan Cai<sup>a,g,1</sup>, Kun Xiong<sup>a,1</sup>, Yaping Chu<sup>b</sup>, Duan-Wu Luo<sup>c</sup>, Xue-Gang Luo<sup>a</sup>, Xian-Yui Yuan<sup>c</sup>, Robert G. Struble<sup>d</sup>, Richard W. Clough<sup>e</sup>, Dennis D. Spencer<sup>f</sup>, Anne Williamson<sup>f</sup>, Jeffrey H. Kordower<sup>b</sup>, Peter R. Patrylo<sup>g</sup>, and Xiao-Xin Yan<sup>e,\*</sup>

<sup>a</sup>Department of Anatomy and Neurobiology, Central South University Xiangya Medical School, Changsha, Hunan 410013, China

<sup>b</sup>Department of Neurological Sciences, Rush University Medical Center, Chicago, IL 60612, USA

<sup>c</sup>Department of Neurosurgery, Central South University Xiangya Hospital, Changsha, Hunan 410078, China

<sup>d</sup>Department of Neurology and Center for Alzheimer Disease, Southern Illinois University School of Medicine, Springfield, IL 62794, USA

<sup>e</sup>Department of Anatomy, Southern Illinois University School of Medicine, Carbondale, IL 62901, USA

<sup>f</sup>Department of Neurosurgery, Yale University School of Medicine, New Haven, CT 06520, USA

<sup>g</sup>Department of Physiology, Southern Illinois University School of Medicine, Carbondale, IL 62901, USA

### Abstract

DCX-immunoreactive (DCX+) cells occur in the piriform cortex in adult mice and rats, but also in the neocortex in adult guinea pigs and rabbits. Here we describe these cells in adult domestic cats and primates. In cats and rhesus monkeys, DCX+ cells existed across the allo- and neocortex, with an overall ventrodorsal high to low gradient at a given frontal plane. Labeled cells formed a cellular band in layers II and upper III, exhibiting dramatic differences in somal size (5–20  $\mu\text{m}$ ), shape (unipolar, bipolar, multipolar and irregular), neuritic complexity and labeling intensity. Cell clusters were also seen in this band, and those in the entorhinal cortex extended into deeper layers as chain-like structures. Densitometry revealed a parallel decline of the cells across regions with age in cats. Besides the cellular band, medium-sized cells with weak DCX reactivity resided sparsely in other layers. Throughout the cortex, virtually all DCX+ cells co-expressed polysialylated neural cell adhesion molecule. Medium to large mature-looking DCX+ cells frequently colocalized with neuron-specific nuclear protein and  $\gamma$ -aminobutyric acid (GABA), and those with a reduced DCX expression also partially co-labeled for glutamic acid decarboxylase, parvalbumin, calbindin,  $\beta$ -nicotinamide adenine dinucleotide phosphate diaphorase and neuronal nitric oxide synthase. Similar to cats and monkeys, small and larger DCX+ cells were detected in surgically removed human frontal and temporal cortices. These data suggest that immature neurons persist into adulthood in many cortical areas in cats and primates, and that these cells appear to undergo development and differentiation to become functional subgroups of GABAergic interneurons.

\*Corresponding author. Department of Anatomy, Southern Illinois University at Carbondale, 1135 Lincoln Drive, #2069 Life Science III, Carbondale, IL 62901-6525, USA. Fax: +1 618 453 6527. xyan@siu.edu (X.-X. Yan).

<sup>1</sup>These authors contributed equally to this work.

## Keywords

Interneurons; GABAergic; Layer II; Neuroplasticity; Corticogenesis

---

## Introduction

Doublecortin (DCX) is a microtubule-associated protein critical for radial and tangential migration of immature neurons in the developing brain (des Portes et al., 1998; Gleeson et al., 1999; Francis et al., 1999; Friocourt et al., 2007). Persistent DCX expression occurs in discrete adult brain regions (Nacher et al., 2001). This adult expression in the subgranular and subventricular zones reflects neurogenic activity giving rise to new granule cells in the hippocampal dentate gyrus and interneurons in the olfactory bulb (Gritti et al., 2002; Couillard-Despres et al., 2005; Gould, 2007). In general, DCX expression in developing neurons declines with cell differentiation and maturation. Therefore, a partial colocalization of DCX with some terminal neuronal markers, e.g., neuron-specific nuclear protein (NeuN), can be detected among a cohort of immature neurons undergoing development (Brown et al., 2003).

Cells concurrently expressing DCX and other immature neuronal markers, e.g., polysialylated neural cell adhesion molecule (PSA-NCAM) and neuron-specific tubulin-III (TuJ1), are reported in layers II/III in mouse/rat piriform cortex (Seki and Arai, 1991; Bonfanti et al., 1992; Nacher et al., 2001), and in primate entorhinal/temporal cortex (Bernier et al., 2002; Tonchev et al., 2003). PSA-NCAM<sup>+</sup> cells are also described in rat and human medial prefrontal cortex (Fox et al., 2000; Sairanen et al., 2007; Varea et al., 2007). These cortical cells were classified as mature neurons undergoing structural plasticity (Nacher et al., 2001), and have been lately clarified as immature neurons (Gómez-Climent et al., 2008). Controversy remains as to whether they are born prenatally (Gómez-Climent et al., 2008) or postnatally (Bernier et al., 2002; Pekcec et al., 2006; Shapiro et al., 2007, 2008).

Unlike mice and rats, DCX<sup>+</sup> cells in adult guinea pigs and rabbits reside in layer II throughout the neocortex in addition to allocortex (Xiong et al., 2008; Luzzati et al., 2008). Therefore, DCX<sup>+</sup> cells might have a wide neocortical distribution in higher mammalian species. To explore this possibility, the present study determined DCX<sup>+</sup> cells in adult domestic cat, rhesus monkey and human cerebral cortex. DCX<sup>+</sup> cells resembling immature and developing neurons were detected in broad cortical areas in these species, with small cells occurring in layers II and upper III and larger ones in all layers. Almost all DCX<sup>+</sup> cells co-expressed PSA-NCAM. Relatively larger DCX<sup>+</sup> cells with mature-looking morphology colocalized with NeuN, and in part with several terminal markers of interneurons, including  $\gamma$ -aminobutyric acid (GABA), glutamic acid decarboxylase (GAD67), parvalbumin (PV), calbindin (CB), and  $\beta$ -nicotinamide adenine dinucleotide phosphate diaphorase (NADPH-d) or neuronal isoform of nitric oxide synthase (nNOS). Collectively, DCX<sup>+</sup> cells likely represent a wave of immature and maturing neurons undergoing development and differentiation into presumably GABAergic subpopulations. Thus, interneuron development may extend beyond puberty to adulthood in many parts of the cerebral cortex in high mammalian species, and this protracted course of interneuron development may be essential for cortical morphogenesis, plasticity and functionality.

## Materials and methods

### Animal and tissue preparation

Domestic cats aged at 15, 17, and 21 months [young adults, male, mean =  $1.5 \pm 0.3$  year-old (yr-old)] and 42, 55, 59 and 62 months (adults, male, mean =  $4.5 \pm 0.7$  yr-old), weighing 2.1–4.3 kg, were obtained from the animal facility of Hunan Agricultural University (Changsha,

Hunan, China). The brains were used to characterize cortical DCX<sup>+</sup> cells including a potential age-related decline of the cells in this species (Xiong et al., 2008). Animals were perfused via the ascending aorta with 4% paraformaldehyde in 0.01 M phosphate-buffered saline (pH 7.4, PBS) under overdose anesthesia (sodium pentobarbital, 100 mg/kg, i.p.). Brains were removed, bisected and postfixed in the perfusion solution overnight, and then soaked in 30% sucrose in PBS at 4 °C until brain blocks sunk. A slice of the temporoparietal cortex (~0.5 cm thick) was prepared from one hemisphere immediately after perfusion and post-fixed with 4% paraformaldehyde together with 1% glutaraldehyde for GABA immunolabeling.

Paraformaldehyde-perfused cerebral hemispheres from three normal rhesus monkeys (*Macaca mulatta*) aged around 12 yr-old (12.1, 12.4 and 12.5 yr) were available from recent studies in primates (e.g., Chu and Kordower, 2007). Cortical blocks were stored in 30% sucrose at 4 °C for a few months before they were examined in the current investigation.

Cerebral hemisphere was cut coronally using a cryostat. Twenty-four consecutive sections (30 μm) were collected into culture plates, and subsets of these sections were used for immunolabeling. Approximately 20 sets of 8 μm sections anterior to the genu of the corpus callosum and near the temporal pole were also collected, and subsets of these latter sections were used for double immunofluorescence. One set of the 30 μm sections was processed with Nissl stain for histological orientation.

Animal use was in accordance with the National Institute of Health Guide for the Care and Use of Laboratory Animals, and was approved by the Ethics Committee of Central South University on Animal Use as well as by Institutional Animal Care and Use Committee of Rush University.

### Human cortical biopsy

Human cortical samples (containing up to 1 × 1 cm<sup>2</sup> cortical surface with underlying grey and white matters) were obtained during surgery of patients with intracranial tumors or recurrent temporal epilepsy (Williamson and Patrylo, 2007), under pre-operative consensus (Table 1). The cortices analyzed in the current study were superficial or peripheral to the tumor/epileptic loci, and lacked any detectable histological abnormality. Cortical biopsies were immediately rinsed with cold saline, immersed in 4% paraformaldehyde in PBS at 4 °C for 24 h, and then stored in 30% sucrose for a few months before cutting (at 30 μm).

### Immunohistochemistry

The goat anti-DCX antibody (sc-8066, Santa Cruz Biotech) has been characterized in multiple species in previous studies (e.g., Brown et al., 2003; Liu et al., 2007; Gómez-Climent et al., 2008; Luzzati et al., 2008; Xiong et al., 2008). We also used two additional DCX antibodies raised in mouse (BD Biosciences) and rabbit (Abcam) (see Table 2), which yielded similar immunolabelings in the cortex, subventricular zone and dentate gyrus, as with the goat antibody (data not shown).

Sections were first treated with 1% H<sub>2</sub>O<sub>2</sub> in PBS for 30 min, and pre-incubated in 5% normal horse serum (NHS) in PBS with 0.3% Triton X-100 for 1 h at room temperature, followed by incubations with anti-DCX antibodies overnight at 4 °C. Sections were further reacted with biotinylated universal secondary antibody at 1:400 for 2 h, and subsequently with ABC reagents (1:400) (Vector Laboratories, Burlingame, CA) for 1 h. Immunoreaction product was visualized using 0.003% hydrogen peroxide and 0.05% diaminobenzidine with (for monkey and human cortex) and without (cat cortex) nickel enhancement (0.025% nickel chloride and 0.025% cobalt chloride). Three 10-minute washes with PBS were used between incubations. Sections were mounted on slides, allowed to air-dry, and coverslipped. Some immunostained

sections were lightly counterstained with cresyl violet to verify laminar distribution of the labeled cells.

For immunofluorescence, thaw-mounted sections (8  $\mu\text{m}$ ) were incubated overnight at 4 °C in PBS containing 5% donkey serum, 0.3% Triton X-100 and a pair of primary antibodies raised in different species at pre-optimized concentrations (Table 2). Sections were then reacted for 2 h with Alexa-Fluor® 488 and Alexa-Fluor® 568 conjugated donkey antibodies against mouse, rabbit or goat IgGs (1:200, Invitrogen, Carlsbad, CA). Sections were finally counterstained with bisbenzimidazole (Hoechst 33342, 1:50,000), washed and coverslipped with anti-fading medium (Vector Laboratories).

### **NADPH-diaphorase histochemistry**

Sections (8  $\mu\text{m}$ ) were incubated in 0.05 M Tris–HCl buffered saline (pH 8.0, TBS) containing 0.3% Triton X-100, 1 mM  $\beta$ -NADPH-d (N7505, Sigma-Aldrich), 0.8 mM nitroblue tetrazolium (N6639, Sigma-Aldrich) and 5% dimethyl sulfoxide for 45 min at 37 °C. The reaction was stopped by rinsing sections in PBS. These sections, together with a set of new sections (i.e., not pre-stained with  $\beta$ -NADPH-d), were immunostained for DCX using the peroxidase method to assess colocalization.

### **Imaging and densitometry**

Immunostained sections were photographed over a light box, and the resulting images were used to create hemispheric cortical maps by tracing along the pial surface and around major neuroanatomic structures. The maps were referred to later during microscopic examination and imaging of labeling in various cortical areas, using an Olympus fluorescent BX60 microscope equipped with a digital imaging system (MicroFire® CCD Camera and software, Optronics, Goleta, CA). Immunofluorescent labelings (in 8  $\mu\text{m}$  sections) were examined with 20 $\times$  and 40 $\times$  objectives using green (DCX labeling), red (other immunolabelings) and blue (bisbenzimidazole stain) fluorescent filters.

Densitometry was carried out in selected cortical areas using three equally distant (360  $\mu\text{m}$  apart) sections per brain at/near the levels of the anterior (frontal lobe) and posterior (occipital lobe) ends of the lateral ventricle, and the dorsal lateral geniculate nucleus (LGNd) (temporoparietal lobe), respectively. The cortical regions chosen for cell count were located around the midpoints between major cerebral sulci/fissures and had a flat pial surface. This landmark-based sampling method assured comparable analysis of cortical areas across brains.

### **Statistical testing and figure preparation**

Means of cell densities were calculated for each cortical area, and for each individual animal. Group means were then calculated and compared using two-way ANOVA with Bonferroni post-tests (Prism GraphPad 4.1, San Diego, CA). The minimal significance level was set at  $p < 0.05$ . All illustrations were prepared with Corel Draw 10 (Ontario, Canada).

## **Results**

### **Distribution of DCX+ cells in young adult cat cortex**

In the frontal lobe sections, DCX+ cells and processes were most dense in the subventricular zone lining the anterior horn of the lateral ventricle (Figs. 1A, B). Upon leaving the ventricular wall, labeled profiles arranged in a curved path that paralleled the white matter, instead of entering the overlying cortex (Fig. 1C). Thus, labeling in this region appeared to represent DCX expression in the subventricular zone-rostral migratory stream, as characterized in other species (Nacher et al., 2001; Gritti et al., 2002; Xiong et al., 2008). Immunoreactive perikarya and neuritic processes were also clearly present within the cortical mantle (Figs. 1A, D–I). A

cellular band composed of immunoreactive somata and processes was evident in layers II and upper III across all the frontal cortical regions assessed, and were most dense at the upper border of layer II. A small number of labeled cells also occurred in other cortical layers (Figs. 1D, F, G, I). The ventral portions of the frontal lobe, including the ventral medial frontal area (VMF) (Figs. 1B, C), dorsal medial prefrontal area (DMP) (Figs. 1D–F) and dorsal lateral prefrontal area (DLP) (Fig. 1H), contained more labeled profiles relative to the dorsal (dorsolateral and dorsomedial) regions of this lobe occupied by the primary somatosensory and motor areas (Fig. 1I).

In the temporoparietal lobe sections, DCX expression was prominent in both the cortex and the subgranular zone (Fig. 2; Supplemental Fig. 1). A clear ventrodorsal (high to low) gradient existed across the cortical hemisphere, especially regarding the abundance of labeled somata and processes in layers II/III. For instance, at the levels of LGNd, labeled profiles were most abundant in the entorhinal cortex but declined when moving towards the temporal, auditory II, auditory I, and finally the primary visual, areas (Supplemental Figs. 1C–G). Similarly, at the level of the medial geniculate body, labeled cells and processes appeared very dense in the entorhinal and adjoining temporal areas, with a noticeable reduction of the labeling in the latter (Figs. 2A, B).

In the occipital lobe sections, a ventrodorsal gradient in the amount of labeling occurred across the visual domain areas. Thus, labeled profiles appeared to decrease in number moving from area 20 (V4), to area 19 (V3), to area 18 (V2), and to area 17 (V1) (Supplemental Figs. 2A–H).

DCX labeling was rare in the subventricular zone and adjacent white matter in proximity to the inferior and posterior horns of the lateral ventricle (Figs. 2A, C, I, J; Supplemental Figs. 2A, B, D), in sharp contrast with the pattern seen around the anterior horn (Figs. 1B, C).

### **Decrease of DCX+ cells with age in cat cortex**

DCX+ cells were detectable in most cortical areas in all of the older adult cats examined in the current study (3.5–5.2 yr-old). However, the abundance of labeling appeared to be reduced in general in these animals relative to young adults, while the overall laminar distribution pattern as well as the ventrodorsal gradient of labeling was largely maintained with age (Fig. 3, Supplemental Fig. 3). Specifically, in the 5.2 yr-old cat (the oldest in this study), the cellular band in layers II/upper III remained visible in the ventromedial and ventrolateral frontal cortical areas (Figs. 3A–G), the entorhinal and low temporal areas (Figs. 3H, K–N) and the ventral occipital regions (areas 20, 19) (not shown). This band was not evident in more dorsal cortical regions (both the lateral and medial aspects), such as S1, A2, A1, V2 and V1, as well as the motor cortex (not shown). However, as in the cortex of young animals, a small number of weakly stained cells remained in most cortical regions (Figs. 3C, D, K–P). Consistent with a global decline of DCX expression in the brain, immunoreactivity in the frontal lobe subventricular zone and hippocampal subgranular zone was dramatically reduced in this adult cat (Figs. 3B, H–J).

Quantitative analysis was carried out to assess cell density in the cellular band over layers II and upper III, which exhibited apparent region and age-related alterations (Fig. 4). A montage of three adjoining 10× images was created for a given cortical region, which was imported as the background layer of a CorelDraw file. To define the vertical distance (depth) of the cellular band in a systematic manner, we used layer I as an internal reference. Thus, the depth of the band was set to be equivalent to that of the overlying layer I in the same area. Dots were created, group-copied and placed one by one on top of individual labeled somata. The background image layer was subsequently deleted, resulting in a map of labeled cells over the area of interest (Figs. 4A–B'). Total area of the band (T), areas occupied by all dots (Tdt) and a single dot (dt)



(i.e., unit area) were measured with Image-J. Cell density was thus calculated based on the formula  $Tdt/dt/T$ , and expressed as number of cells per  $mm^2$ .

An overall decline of DCX+ cells was found between the young and older adult groups of cats across all areas analyzed. As plotted in Fig. 4C, the age-related difference was significant for the frontal areas ( $F = 32$ ,  $DFn = 1$ ,  $DFd = 15$ ), temporoparietal areas ( $F = 64$ ,  $DFn = 1$ ,  $DFd = 20$ ), and the occipital areas ( $F = 48$ ,  $DFn = 1$ ,  $DFd = 20$ ) (with  $p < 0.0001$  in all lobes, two-way ANOVA). Also, there existed an overall difference among the analyzed cortical subregions of the same lobe in both age groups [ $F = 10$  ( $DFn = 1$ ,  $DFd = 15$ ) for three frontal areas,  $F = 11$  ( $DFn = 1$ ,  $DFd = 20$ ), for four temporoparietal areas, and  $F = 14$  ( $DFn = 1$ ,  $DFd = 40$ ) for four visual domain areas,  $p < 0.005$ ]. Of note, the following pair comparisons of means did not reach statistical significance in Bonferroni post-tests: S1 vs motor areas, A2 vs A1, V3 vs V2 or V1, and V2 vs V1 in the adult group, as well as V2 vs V1 in the young adult group (Fig. 4C).

### Overall morphology of DCX+ cells in cat cortex

DBX+ cortical cells in both the young and older adult cats exhibited a heterogeneous morphology largely in a lamina-dependent manner. Within the cellular band over layers II and upper III, DCX+ cells showed a great variability in size, shape, labeling intensity, and number/length/thickness of processes (Figs. 1F; 2D–E; Supplemental Figs. 1H–J; 2I, J). Somal size of the cells ranged from considerably small ( $\sim 5 \mu m$ ) to fairly large (up to  $20 \mu m$ ). The small cells were mostly unipolar or bipolar, whereas larger ones often multipolar and some irregular (Figs. 1F, G; 3G, J, L; 5A–R). Larger cells generally had stronger immunoreactivity, thicker and longer neuritic processes relative to small cells. However, some large cells with well-formed processes exhibited otherwise apparently reduced immunoreactivity (Figs. 1F; 5F, G; Supplemental Figs. 1H, I; 2I).

Other labeled cells exhibited relatively uniform morphology characterized by medium size ( $10\text{--}15 \mu m$ ), round/oval somal shape, weak reactivity and short processes. These cells were found in all cortical layers with a general low density (Figs. 1D, F–I; 2F; 3G, O, P). Moving from ventral to dorsal cortical regions at a given hemispheric level, these medium-sized cells became somewhat more prominent due to the reduced DCX+ cells in layers II/III (Figs. 1H, I; Supplemental Figs. 1D–G; 2E–J; 3G, H). Pilot densitometry failed to detect a statistically significant regional difference of these cells over layers III to VI (temporal lobe regions, young adult group). Therefore, no effort was made to quantify these cells in subsequent analysis.

### Cluster and chain-like arrangements of DCX+ cells in cat cortex

DCX+ cells in layers II/III sometimes arranged as clusters that contained a few or several closely apposed somata (Figs. 1F; 2A–E; 5A–E). Cells within a given cluster often appeared to have comparable morphological characteristics, e.g., similar somal size and shape, staining intensity and neuritic complexity (Figs. 1F; 2C–E; 5A–E). However, in some cases closely apposed cells exhibited dramatic difference in reactivity and morphology (Figs. 1F; 5G, H).

A unique type of cell cluster consisted of small labeled cells and their processes seemingly arranged as migratory chains, which occurred largely in the entorhinal cortex and were most prominent in the young adult cats (Figs. 2; 5I, J). A typical chain structure had an enlarged base located in layer II, and a long chain that became thinner as it extended into deeper layers (as far as layer V). The base was packed with many small cells, some of which appeared to migrate away in a radiation manner, either tangentially or obliquely (towards the white matter). The remainder of the cells appeared to migrate inwardly along the chain, with some voyaging away en route. The proximal portion of the chain (close to the base) was thicker and contained more densely packed cells relative to the distal portion. The latter consisted of a few fusiform

somata that were separated with increasing length of labeled processes, especially towards the end of the chain (Figs. 2C–H; 5I, J).

In older adult cats, there was a dramatic reduction of cells associated with a given chain structure (Figs. 3H, K, L; Supplemental Figs. 3D–F). As a result, the base of the chain in layer II became much smaller or no longer impressive. Also, in most parts of the chain labeled somata and processes were aligned as a single array. As with those in young adult cats, cells appeared to migrate away from the chain in the proximal or distal portions. Cells that had left the chain appeared somewhat larger in size and exhibited weaker reactivity relative to their counterparts remaining on the chain (Fig. 3L; Supplemental Fig. 3F).

### **Colocalization of immature and mature neuronal markers in DCX+ cells in cat cortex**

Double labeling was carried out in the cat cortex to assess DCX colocalization with other neuronal and glial markers similar to our recent characterization of these cells in guinea pigs (Xiong et al., 2008). DCX+ cells in layers II–III exhibited virtually a complete colocalization with PSA-NCAM (Figs. 5A–E) and TuJ1 (not shown).

NeuN and GABA were differentially expressed among DCX+ cells (Figs. 5F–M). Thus, small unipolar and bipolar DCX+ cells, including those arranged in clusters and chain-like formations, did not exhibit NeuN or GABA reactivity. In contrast, medium to large DCX+ cells in bipolar and multipolar shapes and with well-developed neuritic processes consistently co-expressed NeuN and GABA. Of note, all medium-sized DCX+ cells, including those located deep to the cellular band in layers II/III, displayed clear colocalization with NeuN and GABA (Figs. 5F, K–M). A clear transition in relative levels of DCX and NeuN could be found among a group of cells within a local area. Thus, DCX levels appeared to increase as the cells became larger and had more and thicker neuritic processes. However, DCX levels attenuated as the cells became even more mature-looking, in parallel with emergence and elevation of NeuN (Fig. 5F).

Medium and large-sized cells with attenuated DCX reactivity were specifically found to colocalize partially with several other terminal markers of interneurons. Thus, DCX+/GAD67+ cells occurred in layers II/III as well as in deeper layers (Figs. 5O–R), as were DCX+/CB+ cells (Figs. 6A–E). DCX+/PV+ cells were found in layers II/III but not in deep cortical layers, with DCX reactivity in these double-labeled cells being faint or very weak (Figs. 6F–H). No DCX and CR double-labeled cells were found in the present study (Figs. 6I–K). Colocalization of NADPH-d or nNOS appeared to be considerably common in medium-sized cells with weak DCX reactivity localized to the cellular band over layers II and upper III as well as the remainder of the cortex (Fig. 7). In fact, DCX+/NADPH-d+ cells were also found in layer I (not shown). All of these double-labeled cells were type II NADPH-d neurons (Yan et al., 1996b; Estrada and DeFelipe, 1998; Garbossa et al., 2005). Of note, DCX+/NADPH-d+ cells appeared somewhat smaller than neighboring type II neurons that lacked DCX but exhibited stronger NADPH-d reaction (Figs. 7A–F).

Some medium-sized DCX+ cells in layers III–V also colocalized with somatostatin (SOM) (Varea et al., 2007). No DCX+ cells were found to express neurogranin, a marker of pyramidal neurons (Xiong et al., 2008). Labelings for GFAP (astrocytes), OX42 (microglia) and oligodendrocyte-specific protein, were not detected in any DCX+ cell (data not shown).

### **Presence of similar DCX+ cells in adult monkey and human cortex**

Morphologically heterogeneous DCX+ cells were observed in layers II and upper III in most cortical areas of all the monkeys examined (Fig. 8). In the frontal lobe, a cellular band at this location appeared in the ventral and medial cortical regions especially the prefrontal areas

(Figs. 8A–D), whereas individual labeled somata were detectable in the remaining regions (not shown). Most labeled cells were bipolar but some multipolar. Larger and weakly stained cells were visible in deeper cortical layers (Figs. 8B, D). In the temporoparietal cortex, numerous cells occurred in the entorhinal area, and they arranged as large clusters seemingly associated with the island formations of layer II (Fig. 8G). Labeled profiles formed virtually a continuous band in layers II/upper III throughout the temporal gyri (Figs. 8A, H, I, M), which extended dorsally into the insular and adjoining parietal cortex, with an apparently reduced cell density (Figs. 8A, J, K). A few labeled cells occurred further dorsally in the primary somatosensory and motor areas (Figs. 8A, L). In the occipital lobe, a few cells were encountered over layer II in areas 17, whereas more cells at this lamina occurred in the associative visual areas peripheral to the striate cortex (not shown). Moderate DCX expression was present in the dentate subgranular zone of these monkeys (Figs. 8E, F).

DCX+ cells were detectable in the cortex of all human specimens examined in this study (Fig. 9). Labeled cells at the upper border of layer II varied considerably in somal size and shape, staining intensity and neuritic appearance, with small bipolar and a few multipolar cells exhibited heavy reactivity (Figs. 9A–H, K–M). Medium-sized cells with weak to moderate reactivity were found in layers II–VI (mostly in II–IV) (Figs. 9I, J). Because the density of labeled cells varied greatly between cases, no quantitative analysis was included in the current study.

## Discussion

DCX or PSA-NCAM+ cells occur in the piriform and medial prefrontal cortices in small laboratory rodents (Seki and Arai, 1991; Fox et al., 2000; Nacher et al., 2001; Sairanen et al., 2007). These cells are reported or have been noticed in the neocortex as well in larger mammals, including guinea pigs (Xiong et al., 2008; Luzzati et al., 2008), rabbits (Luzzati et al., 2008), cats (Gómez-Climent et al., 2008), monkeys (Bernier et al., 2002; Kornack et al., 2005), and humans (Varea et al., 2007; Liu et al., 2007). Their cellular identity, origin and fate, as well as the extent and implication of their species differences, remain to be determined.

### Phenotype and fate of DCX+ cortical cells

We recently propose DCX+ cells in guinea pig cortex as immature and developing neurons (Xiong et al., 2008). This notion is supported by two later studies of these cells in adult rats (Gómez-Climent et al., 2008), and in adult guinea pigs and rabbits (Luzzati et al., 2008). DCX+ cortical cells in adult cats and primates exhibit a great morphological diversity, with somal size ranging from small, medium to large, and shape from unipolar, bipolar, multipolar to irregular. DCX levels also vary among cells, with an attenuated expression in more mature-looking neurons. Moreover, these mature-looking cells co-express NeuN, GABA/GAD, and specific markers of interneuron subgroups including CB, PV, NADPH-d and nNOS. The simplest explanation for such a dynamic morphological and neurochemical spectrum among the DCX+ cells is that they as a whole are a cohort of immature and maturing neurons. Thus, the small DCX+ cells that do not express any mature markers represent the “infant” or immature members of the cohort. They develop and differentiate into transitional or young neurons that start to express specific interneuron markers. This notion fits with recent understanding on successive expressions of immature and mature markers during neuronal development (Brown et al., 2003). Therefore, DCX+ cells would likely contribute at least PV, CB and type II nitric oxide-producing GABAergic subgroups to postnatal cortex.

In general, the small cells occur in layers II/upper III, while larger ones localize to deeper layers besides II/III. Thus, most DCX+ cells might undergo intracortical migration outside-in, in parallel with morphological maturation. In fact, many small cells in the entorhinal cortex appear to voyage from layer II to deeper locations in a chain-like migration manner. Of note, medium



and large-sized cells may coexist with the small ones within layers II/III. A few medium-sized cells also occur in layer I. Therefore, small DCX+ cells in layers II/III also appear to develop and mature locally, and some might migrate into layer I.

### Origin of DCX+ cortical cells

It is currently under debate whether these cortical DCX+ cells in various species might be adult-born. Several studies show BrdU incorporation in some DCX+ cells in rodent and primate piriform cortex (Bernier et al., 2002; Tonchev et al., 2003; Pekcec et al., 2006; Shapiro et al., 2007, 2008). In contrast, other studies report no BrdU incorporation into these cells in postnatal rats, guinea pigs and rabbits (Gómez-Climent et al., 2008; Luzzati et al., 2008). Of note, a total of 100% PSA-NCAM+ cells was co-labeled with BrdU in the piriform cortex of 3 month-old rats following administration of this S-phase marker at embryonic days 11.5, 13.5 and 15.5 (Gómez-Climent et al., 2008). We are in favor of a likelihood that DCX+ neurons in adult cat and primate cortex are generated at earlier, prenatal or postnatal, stages.

It is also unclear where these DCX+ cortical cells originate from. It has been suggested that in rodent and primate piriform and temporal cortex these cells derive from the subventricular zone (Bernier et al., 2002; Pekcec et al., 2006; Shapiro et al., 2007, 2008). However, there is little DCX labeling around the ventricular region or white matter in most cortical areas in cats and monkeys, nor any band-like arrangement of labeling indicative of outward cell migration in the cortex. DCX+ profiles around the anterior horn appear to migrate away from the ventricle, but they essentially join the rostral migratory stream instead of entering the cortex.

Evidence from small laboratory rodents indicates that interneurons originate largely from subpallial structures, with their precursors entering the cortex by tangential migration including via layer I. These precursors then descend to and populate over the cortical plate (Soriano et al., 1992; Lavdas et al., 1999; Wichterle et al., 1999; Ang et al., 2003; Hevner et al., 2004). However, evidence from primates suggests more complicated origins of cortical interneurons, including (although often neglected) pallial sources, e.g., the ventricular and marginal zones, and the subpial granular layer (Zecevic and Rakic, 2001; DeFelipe, 2002; Letinic et al., 2002; Rakic and Zecevic, 2003; Petanjek et al., 2008). In fact, the marginal zone/layer I may serve a neurogenic niche for GABAergic interneurons in rats (Costa et al., 2007). Thus, DCX + cortical cells might derive from interneuron precursors intrinsic to layer I or those arrived in this layer by tangential migration. This notion would reconcile some aspects of these cells, including their lamination and clusterization at layer II, potential to develop into GABAergic subgroups, and a pattern of inward migration for most cells.

### Protracted DCX expression and its relevance to interneuron development

DCX+ cells in cat cortex evolve with time and location. In layers II/III these cells exhibit a distinct ventrodorsal gradient from high to low density across the cerebral hemisphere at a given brain level in young adult cats. This cellular band appears to “retract” dorsoventrally with age. In the oldest cat (5.2 yr-old) examined, this band is largely restricted to the entorhinal and adjoining temporal cortex. In ~12-yr old monkeys, this band still extends across most hemispheric regions. In adult humans, small and medium-sized DCX+ cells with strong to weak reactivity exist in layer II in the frontal and temporal neocortex. Many medium-sized cells with weak DCX reactivity remain in more dorsally located areas in older adult cats, wherein the layers II/III cellular band has disappeared. These medium cells are seen over the adult monkey and human cortices examined in this study.

In general, CB+ and PV+ non-pyramidal neurons may develop over a fairly long postnatal period in cat and primate cortex (Stichel et al., 1987; Hogan et al., 1992; Alcántara and Ferrer, 1994; 1995; Cruz et al., 2003). Type II NADPH-d neurons, a potential major destiny of DCX

+ cells, might also develop late in mammalian cortex. In human cortex they are few before birth (Yan et al., 1996a, Yan and Ribak, 1997), yet considerably abundant in the adult (Judas et al., 1999; Garbossa et al., 2005; Koliatsos et al., 2006). Of note, CB+ and PV+ interneurons appear to emerge later in the limbic and associative relative to primary cortical areas. They occur long before birth in monkey and human striate cortex (Hendrickson et al., 1991; Cao et al., 1996; Yan et al., 1997a), but several months after birth in the entorhinal and prefrontal areas (Reynolds and Beasley, 2001; Erickson and Lewis, 2002; Grateron et al., 2003). Thus, the ventrodorsal gradient of DCX+ cells and its evolution with age might reflect an order of interneuron development across regions, particularly in accordance with a protracted interneuron development in the limbic and associative areas.

### Species difference of DCX+ cortical cells

As aforementioned, there exists a remarkable difference between mice/rats and larger mammals regarding the presence of DCX+ cells in the neocortex (Gómez-Clement et al., 2008; Luzzati et al., 2008). This interspecies difference of DCX+ cells seems to match with that of type II NADPH-d neurons (Yan et al., 1996b, Yan and Garey, 1997; Gabbott and Bacon, 1995; Judas et al., 1999; Smiley et al., 2000; Garbossa et al., 2005; Koliatsos et al., 2006). Also, it appears that DCX+ cells in cats and primates may occur over broader cortical layers and display more distinct colocalization with various mature interneuron markers relative to their counterparts in smaller mammals (Varea et al., 2007; Xiong et al., 2008; Gómez-Clement et al., 2008; Luzzati et al., 2008).

Evidence suggests that cortical expansion during mammalian evolution, including emergence and specification of high order associative areas, parallels an increased number and diversity of GABAergic neurons (Jones, 1993; DeFelipe, 2002; Letinic et al., 2002; Petanjek et al., 2008). This change in interneuron system might be achieved through a boosting of preexisting cellular mechanism and/or extension of developmental program (Luzzati et al., 2008; Petanjek et al., 2008). With this regard, the interspecies difference of cortical DCX+ cells and a prolonged presence of these cells in higher mammals might be relevant to the increase and diversification of cortical interneurons with phylogeny.

In summary, this study extends our previous characterization of cortical DCX+ cells in guinea pigs to cats and primates. We elaborate the nature and implication of persistent DCX expression in ontogenetic and phylogenetic perspective, largely involving interneuron development. The data point to a cellular basis potentially under-pinning normal and certain aberrant interneuron plasticity in mammalian cortex under physiological and perhaps some pathophysiological conditions during development and at adulthood.

### Supplementary Material

Refer to Web version on PubMed Central for supplementary material.

### Acknowledgments

This study was supported in part by Southern Illinois University School of Medicine and Illinois Department of Public Health (X.X.Y.), Xiangya Medical School (Y.C., X.K.) and National Institute of Health (1R21NS056371 to P.R.P., X.X.Y. and NS054038 to A.W).

### Appendix A. Supplementary data

Supplementary data associated with this article can be found, in the online version, at doi: 10.1016/j.expneurol.2008.12.008.

## References

- Alcántara S, Ferrer I. Postnatal development of parvalbumin immunoreactivity in the cerebral cortex of the cat. *J. Comp. Neurol* 1994;348:133–149. [PubMed: 7814682]
- Alcántara S, Ferrer I. Postnatal development of calbindin-D28k immunoreactivity in the cerebral cortex of the cat. *Anat. Embryol. (Berl)* 1995;192:184–369.
- Ang ES, Haydar TF, Gluncic V, Rakic P. Four-dimensional migratory coordinates of GABAergic interneurons in the developing mouse cortex. *J. Neurosci* 2003;23:5805–5815. [PubMed: 12843285]
- Bonfanti L, Olive S, Poulain DA, Theodosis DT. Mapping of the distribution of polysialylated neural cell adhesion molecule throughout the central nervous system of the adult rat: an immunohistochemical study. *Neuroscience* 1992;49:419–436. [PubMed: 1436474]
- Bernier PJ, Bedard A, Vinet J, Levesque M, Parent A. Newly generated neurons in the amygdala and adjoining cortex of adult primates. *Proc. Natl. Acad. Sci. U. S. A* 2002;99:11464–11469. [PubMed: 12177450]
- Brown JP, Couillard-Despres S, Cooper-Kuhn CM, Winkler J, Aigner L, Kuhn HG. Transient expression of doublecortin during adult neurogenesis. *J. Comp. Neurol* 2003;467:1–10. [PubMed: 14574675]
- Cao QL, Yan XX, Luo XG, Garey LJ. Prenatal development of parvalbumin immunoreactivity in the human striate cortex. *Cereb. Cortex* 1996;6:620–630. [PubMed: 8670687]
- Chu Y, Kordower JH. Age-associated increases of alpha-synuclein in monkeys and humans are associated with nigrostriatal dopamine depletion: is this the target for Parkinson's disease? *Neurobiol. Dis* 2007;25:134–149. [PubMed: 17055279]
- Costa MR, Kessaris N, Richardson WD, Götz M, Hedin-Pereira C. The marginal zone/layer I as a novel niche for neurogenesis and gliogenesis in developing cerebral cortex. *J. Neurosci* 2007;27:11376–11388. [PubMed: 17942732]
- Couillard-Despres S, Winner B, Schaubeck S, Aigner R, Vroemen M, Weidner N, Bogdahn U, Winkler J, Kuhn HG, Aigner L. Doublecortin expression levels in adult brain reflect neurogenesis. *Eur. J. Neurosci* 2005;21:1–14. [PubMed: 15654838]
- Cruz DA, Eggan SM, Lewis DA. Postnatal development of pre- and postsynaptic GABA markers at chandelier cell connections with pyramidal neurons in monkey prefrontal cortex. *J. Comp. Neurol* 2003;465:385–400. [PubMed: 12966563]
- DeFelipe J. Cortical interneurons: from Cajal to 2001. *Prog. Brain Res* 2002;136:215–238. [PubMed: 12143384]
- des Portes V, Pinard JM, Billuart P, Vinet MC, Koulakoff A, Carrie A, Gelot A, Dupuis E, Motte J, Berwald-Netter Y, Catala M, Kahn A, Beldjord C, Chelly J. A novel CNS gene required for neuronal migration and involved in X-linked subcortical laminar heterotopia and lissencephaly syndrome. *Cell* 1998;92:51–61. [PubMed: 9489699]
- Erickson SL, Lewis DA. Postnatal development of parvalbumin- and GABA transporter-immunoreactive axon terminals in monkey prefrontal cortex. *J. Comp. Neurol* 2002;448:186–202. [PubMed: 12012429]
- Estrada C, DeFelipe J. Nitric oxide-producing neurons in the neocortex: morphological and functional relationship with intraparenchymal microvasculature. *Cereb. Cortex* 1998;8:193–203. [PubMed: 9617914]
- Fox GB, Fichera G, Barry T, O'Connell AW, Gallagher HC, Murphy KJ, Regan CM. Consolidation of passive avoidance learning is associated with transient increases of polysialylated neurons in layer II of the rat medial temporal cortex. *J. Neurobiol* 2000;45:135–141. [PubMed: 11074459]
- Francis F, Koulakoff A, Boucher D, Chafey P, Schaar B, Vinet MC, Friocourt G, McDonnell N, Reiner O, Kahn A, McConnell SK, Berwald-Netter Y, Denoulet P, Chelly J. Doublecortin is a developmentally regulated, microtubule-associated protein expressed in migrating and differentiating neurons. *Neuron* 1999;23:247–256. [PubMed: 10399932]
- Friocourt G, Liu JS, Antypa M, Rakic S, Walsh CA, Parnavelas JG. Both doublecortin and doublecortin-like kinase play a role in cortical interneuron migration. *J. Neurosci* 2007;27:3875–3883. [PubMed: 17409252]

- Gabbott PL, Bacon SJ. Co-localisation of NADPH diaphorase activity and GABA immunoreactivity in local circuit neurones in the medial prefrontal cortex (mPFC) of the rat. *Brain Res* 1995;699:321–328. [PubMed: 8616637]
- Garbossa D, Fontanella M, Tomasi S, Ducati A, Vercelli A. Differential distribution of NADPH-diaphorase histochemistry in human cerebral cortex. *Brain Res* 2005;1034:1–10. [PubMed: 15713254]
- Gleeson JG, Lin PT, Flanagan LA, Walsh CA. Doublecortin is a microtubule-associated protein and is expressed widely by migrating neurons. *Neuron* 1999;23:257–271. [PubMed: 10399933]
- Gómez-Climent MA, Castillo-Gómez E, Varea E, Guirado R, Blasco-Ibáñez JM, Crespo C, Martínez-Guijarro FJ, Nacher J. A population of prenatally generated cells in the rat paleocortex maintains an immature neuronal phenotype into adulthood. *Cereb. Cortex* 2008;18:2229–2240. [PubMed: 18245040]
- Gould E. How widespread is adult neurogenesis in mammals? *Nat. Rev. Neurosci* 2007;8:481–488. [PubMed: 17514200]
- Grateron L, Cebada-Sanchez S, Marcos P, Mohedano-Moriano A, Insausti AM, Muñoz M, Arroyo-Jimenez MM, Martinez-Marcos A, Artacho-Perula E, Blairot X, Insausti R. Postnatal development of calcium-binding proteins immunoreactivity (parvalbumin, calbindin, calretinin) in the human entorhinal cortex. *J. Chem. Neuroanat* 2003;26:311–316. [PubMed: 14729133]
- Gritti A, Bonfanti L, Doetsch F, Caille I, Alvarez-Buylla A, Lim DA, Galli R, Verdugo JM, Herrera DG, Vescovi AL. Multipotent neural stem cells reside into the rostral extension and olfactory bulb of adult rodents. *J. Neurosci* 2002;22:437–445. [PubMed: 11784788]
- Hendrickson AE, Van Brederode JF, Mulligan KA, Celio MR. Development of the calcium-binding protein parvalbumin and calbindin in monkey striate cortex. *J. Comp. Neurol* 1991;307:626–646. [PubMed: 1651352]
- Hevner RF, Daza RA, Englund C, Kohtz J, Fink A. Postnatal shifts of interneuron position in the neocortex of normal and reeler mice: evidence for inward radial migration. *Neuroscience* 2004;124:605–618. [PubMed: 14980731]
- Hogan D, Terwilleger ER, Berman NE. Development of subpopulations of GABAergic neurons in cat visual cortical areas. *Neuroreport* 1992;3:1069–1072. [PubMed: 1493219]
- Jones EG. GABAergic neurons and their role in cortical plasticity in primates. *Cereb. Cortex* 1993;3:361–372. [PubMed: 8260806]
- Judas M, Sestan N, Kostovic I. Nitrinergic neurons in the developing and adult human telencephalon: transient and permanent patterns of expression in comparison to other mammals. *Microsc. Res. Tech* 1999;45:401–419. [PubMed: 10402267]
- Koliatsos VE, Kecojevic A, Troncoso JC, Gastard MC, Bennett DA, Schneider JA. Early involvement of small inhibitory cortical interneurons in Alzheimer's disease. *Acta Neuropathol* 2006;112:147–162. [PubMed: 16758165]
- Kornack DR, Kelly EA, Shannon DE. Persistent doublecortin expression identifies a novel neuronal population in adult primate neocortex. *Soc. Neurosci. 2005 Abstr.* 143.10.
- Lavdas AA, Grigoriou M, Pachnis V, Parnavelas JG. The medial ganglionic eminence gives rise to a population of early neurons in the developing cerebral cortex. *J. Neurosci* 1999;19:7881–7888. [PubMed: 10479690]
- Letinic K, Zoncu R, Rakic P. Origin of GABAergic neurons in the human neocortex. *Nature* 2002;417:645–649. [PubMed: 12050665]
- Liu Y, Mee E, Bergin P, Teoh HH, Connor B, Dragunow M, Faull RLM. Increased numbers of doublecortin positive cells in the temporal cortex of the adult epileptic human brain. *Soc. Neurosci. 2007 Abstr.* 259.6.
- Luzzati F, Bonfanti L, Fasolo A, Peretto P. DCX and PSA-NCAM expression identifies a population of neurons preferentially distributed in associative areas of different pallial derivatives and vertebrate species. *Cereb. Cortex.* 2008 doi:10.1093/cercor/bhn145.
- Nacher J, Crespo C, McEwen BS. Doublecortin expression in the adult rat telencephalon. *Eur. J. Neurosci* 2001;14:629–644. [PubMed: 11556888]
- Pekcec A, Loscher W, Potschka H. Neurogenesis in the adult rat piriform cortex. *Neuroreport* 2006;17:571–574. [PubMed: 16603913]

- Petanjek Z, Dujmović A, Kostović I, Esclapez M. Distinct origin of GABAergic neurons in forebrain of man, nonhuman primates and lower mammals. *Coll. Antropol* 2008;32(Suppl. 1):9–17. [PubMed: 18405052]
- Rakic S, Zecevic N. Emerging complexity of layer I in human cerebral cortex. *Cereb. Cortex* 2003;3:1072–1083. [PubMed: 12967924]
- Reynolds GP, Beasley CL. GABAergic neuronal subtypes in the human frontal cortex—development and deficits in schizophrenia. *J. Chem. Neuroanat* 2001;22:95–100. [PubMed: 11470557]
- Sairanen M, O’Leary OF, Knuutila JE, Castren E. Chronic antidepressant treatment selectively increases expression of plasticity-related proteins in the hippocampus and medial prefrontal cortex of the rat. *Neuroscience* 2007;144:368–374. [PubMed: 17049169]
- Seki T, Arai Y. Expression of highly polysialylated NCAM in the neocortex and piriform cortex of the developing and the adult rat. *Anat. Embryol. (Berl)* 1991;184:395–401. [PubMed: 1952111]
- Shapiro LA, Ng KL, Kinyamu R, Whitaker-Azmitia P, Geisert EE, Blurton-Jones M, Zhou QY, Ribak CE. Origin, migration and fate of newly generated neurons in the adult rodent piriform cortex. *Brain Struct. Funct* 2007;212:133–148. [PubMed: 17764016]
- Shapiro LA, Ng K, Zhou QY, Ribak CE. Subventricular zone-derived, newly generated neurons populate several olfactory and limbic forebrain regions. *Epilepsy Behav.* 2008 doi:10.1016/j.yebeh.2008.09.011.
- Smiley JF, McGinnis JP, Javitt DC. Nitric oxide synthase interneurons in the monkey cerebral cortex are subsets of the somatostatin, neuropeptide Y, and calbindin cells. *Brain Res* 2000;863:205–212. [PubMed: 10773208]
- Soriano E, Del Rio JA, Ferrer I, Auladell C, De Lecea L, Alcantara S. Late appearance of parvalbumin-immunoreactive neurons in the rodent cerebral cortex does not follow an ‘inside-out’ sequence. *Neurosci. Lett* 1992;142:147–150. [PubMed: 1454208]
- Stichel CC, Singer W, Heizmann CW, Norman AW. Immunohistochemical localization of calcium-binding proteins, parvalbumin and calbindin-D 28k, in the adult and developing visual cortex of cats: a light and electron microscopic study. *J. Comp. Neurol* 1987;262:563–577. [PubMed: 3667965]
- Tonchev AB, Yamashima T, Zhao L, Okano HJ, Okano H. Proliferation of neural and neuronal progenitors after global brain ischemia in young adult macaque monkeys. *Mol. Cell Neurosci* 2003;23:292–301. [PubMed: 12812760]
- Varea E, Castillo-Gomez E, Gomez-Climent MA, Blasco-Ibanez JM, Crespo C, Martinez-Guijarro FJ, Nacher J. PSA-NCAM expression in the human prefrontal cortex. *J. Chem. Neuroanat* 2007;33:202–209. [PubMed: 17467233]
- Wichterle H, Garcia-Verdugo JM, Herrera DG, Alvarez-Buylla A. Young neurons from medial ganglionic eminence disperse in adult and embryonic brain. *Nat. Neurosci* 1999;2:461–466. [PubMed: 10321251]
- Williamson A, Patrylo PR. Physiological studies of human dentate granule cells. *Prog. Brain Res* 2007;163:183–198. [PubMed: 17765719]
- Xiong K, Luo DW, Patrylo PR, Luo XG, Struble RG, Clough RW, Yan XX. Doublecortin-expressing cells are present in layer II across the adult guinea pig cerebral cortex: partial colocalization with mature interneuron markers. *Exp. Neurol* 2008;211:271–282. [PubMed: 18378231]
- Yan XX, Garey LJ. Morphological diversity of nitric oxide synthesising neurons in mammalian cerebral cortex. *J. Hirnforsch* 1997;38:165–172. [PubMed: 9176729]
- Yan XX, Ribak CE. Prenatal development of nicotinamide adenine dinucleotide-diaphorase activity in the human hippocampal formation. *Hippocampus* 1997;7:215–231. [PubMed: 9136051]
- Yan XX, Garey LJ, Jen LS. Prenatal development of NADPH-diaphorase-reactive neurons in human frontal cortex. *Cereb. Cortex* 1996a;6:737–745. [PubMed: 8921208]
- Yan XX, Jen LS, Garey LJ. NADPH-diaphorase-positive neurons in primate cerebral cortex colocalize with GABA and calcium-binding proteins. *Cereb. Cortex* 1996b;6:524–529. [PubMed: 8670678]
- Yan XX, Cao QL, Luo XG, Garey LJ. Prenatal development of calbindin D-28K in human visual cortex. *Cereb. Cortex* 1997a;7:57–62. [PubMed: 9023432]
- Zecevic N, Rakic P. Development of layer I neurons in the primate cerebral cortex. *J. Neurosci* 2001;21:5607–5619. [PubMed: 11466432]



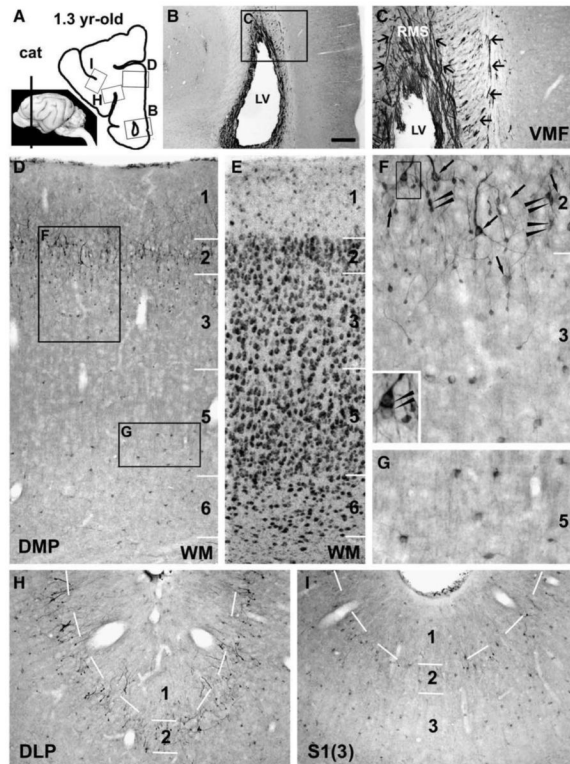


**Fig. 1.**

Doublecortin immunoreactive (DCX+) profiles in the frontal cortical areas in a 1.3 yr-old cat, as marked on the cerebral map in panel A. Panels B and C illustrate heavy labeling in the subventricular zone around the anterior horn of the lateral ventricle (LV). Note that labeled cells and processes do not invade the cortex but largely contribute to the rostral migratory stream (RMS) (arrows, C). Panels D–G show laminar distribution and closer views of DCX+ cells in the agranular (E, Nissl stain) dorsal medial prefrontal area (DMP). Labeled cells are densely distributed in layers II and upper III as a cellular band (D). These cells vary in size and shape, with most of them being small unipolar and bipolar, while some larger and multipolar (F). Labeling intensity also varies among both the small and large (arrows, F) cells. Also, cells with similar or different morphology may arrange as clusters (arrowheads, F). Panels H and I depict labelings over the upper portion of the cortex in the dorsal lateral prefrontal (DLP) and primary somatosensory (S1, area 3) areas, respectively. Note the reduced density of labeled profiles in the layers II/III cellular band in (H) and (I) relative to (D), and in (I) relative to (H). Overall, a population of medium-sized cells with light to moderate DCX reactivity occurs across the cortical depth with a general low density. They become somewhat prominent in S1 (I) relative to DLP (H) and DMP (D), in parallel with reduced cell density in layers II/III. Some of these medium-sized cells are present in layer I, also more noticeable in S1 relative to DLP and DMP. Cortical layers are indicated with Arab numbers and short bars (same for the remaining figures). Scale bar = 450  $\mu$ m in B; equal to 150  $\mu$ m for C, D, E, H, I; 50  $\mu$ m for F, G and 25  $\mu$ m for the low left insert in F.

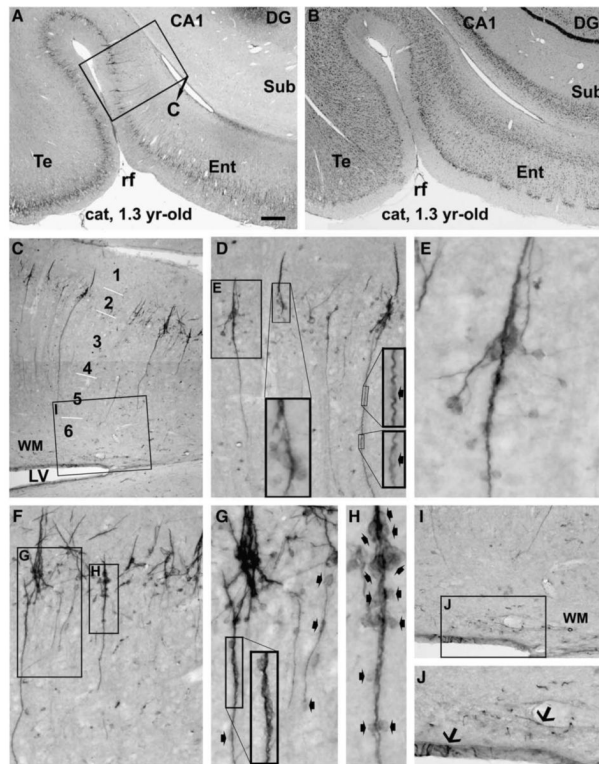


**Fig. 2.** Doublecortin labeling in the entorhinal and adjoining temporal cortex of a young adult cat, focusing on clusters and chain-like formations. Panels A and B are low power views of immunolabeling and Nissl stain, respectively. Immunolabeled profiles in the framed area in (A) are enlarged through (C–H). The clusters are consisted of densely packed small cells. They reside at the border of layers I and II, and many of them form the bases of migratory cells (D, F). Many cells appear to migrate away from the base in a radiation manner (E, G), other cells and processes arrange as chains extending inwardly as far as layer V even VI. For a given chain, cells (small fat arrows) line up tightly in the proximal segment, but are separated by processes in the distal segment with increasing distance towards the end of the chain (F, G). A short arm extends from the base into layer I, which is consisted of immunoreactive processes but not somata (D–F). Panels I and J show a few labeled cells (arrows) in the ventricular wall and adjacent white matter (WM). Scale bar = 600  $\mu$ m in A applying to B; equal to 200  $\mu$ m for C; 100  $\mu$ m for D, F, I; 50  $\mu$ m for G, J and 25  $\mu$ m for E, H.

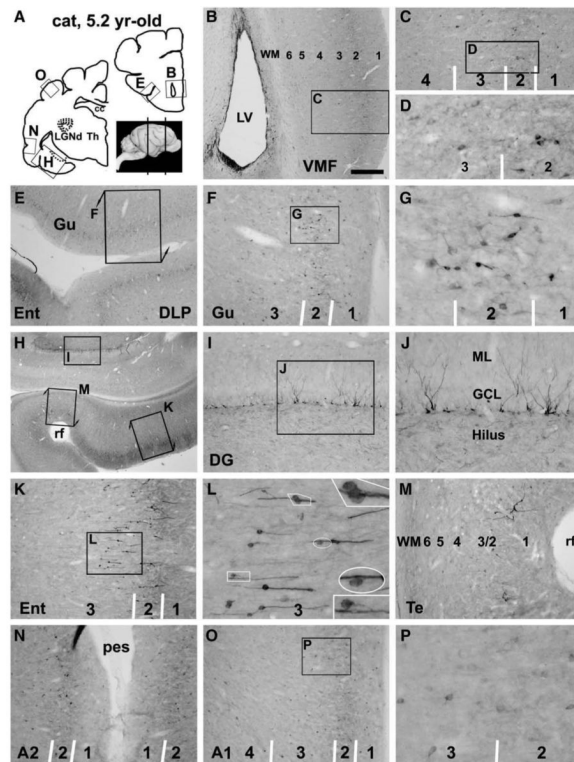


**Fig. 3.**

Doublecortin immunoreactive (DCX+) cells in representative forebrain areas in a 5.2 yr-old cat, as indicated in panel A. Panels B–G illustrate occurrence of some DCX+ cells in the ventral frontal areas, mostly in layers II/III. These cells are in bipolar or multipolar shape, range from small to medium size with distinct to weak reactivity (D, G). Note the reduced immunolabeling in the subventricular zone lining the anterior horn (B), relative to Fig. 1C. Panel H–M show labeled profiles in the dentate gyrus and the transitional area between the entorhinal and temporal cortices. Some DCX+ granule cells are present in the dentate gyrus with their cell bodies located at the subgranular zone (I, J). Small to medium-sized cells are present over layers II–III in the entorhinal cortex, mainly arranged as radially oriented chains. Some cells appear to leave the chain and migrate towards deeper locations (L, with enlarged areas as inserts). Both distinctly and lightly stained DCX+ cells remain in the low temporal (M) and auditory II (N) areas with low density. In more dorsally located auditory I area, only a small number of weakly labeled cells (medium-size) are present (O, P). Scale bar = 750  $\mu$ m in B applying to E, equal to 1.5 mm for H, 300  $\mu$ m for C, F, I, K, M–O; 100  $\mu$ m for D, G, L, P and 33  $\mu$ m for the enlarged inserts in L.

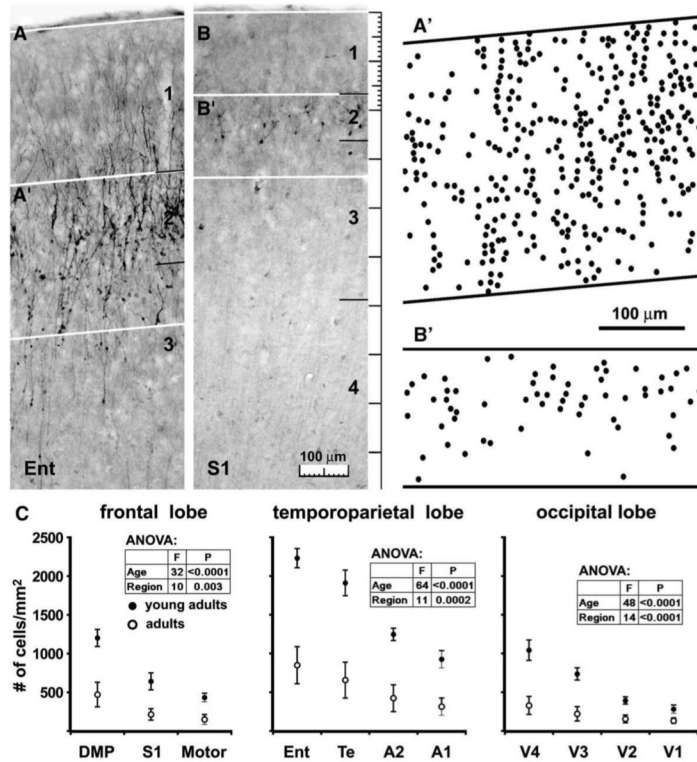


**Fig. 4.** Quantitative analyses of DCX+ cell density over the cellular band in layers II and upper III in selected cortical areas in young (mean age= 1.5 ± 0.3 yr-old) and older (4.5 ± 0.7 yr-old) adult cats. Panels A–B' illustrate the methodology of densitometry using portions of the entorhinal (A) and primary somatosensory (B) areas as examples (from a 1.8 yr-old cat). The radial distance (depth) of the cellular band is defined to be equivalent to that of the overlying layer I in the same area (A, B). Labeled somata in this band are reproduced into a cellular map (A', B'), followed by quantification and statistical analyses (C). Cell densities are reduced in all measured areas in the frontal, temporoparietal and occipital lobes in the young relative to older adult groups. There also exists a general reduction of cell density from ventral to dorsal areas in the same lobe in both age groups, reflecting the visually detected ventrodorsal gradient of DCX labeling across the hemisphere.



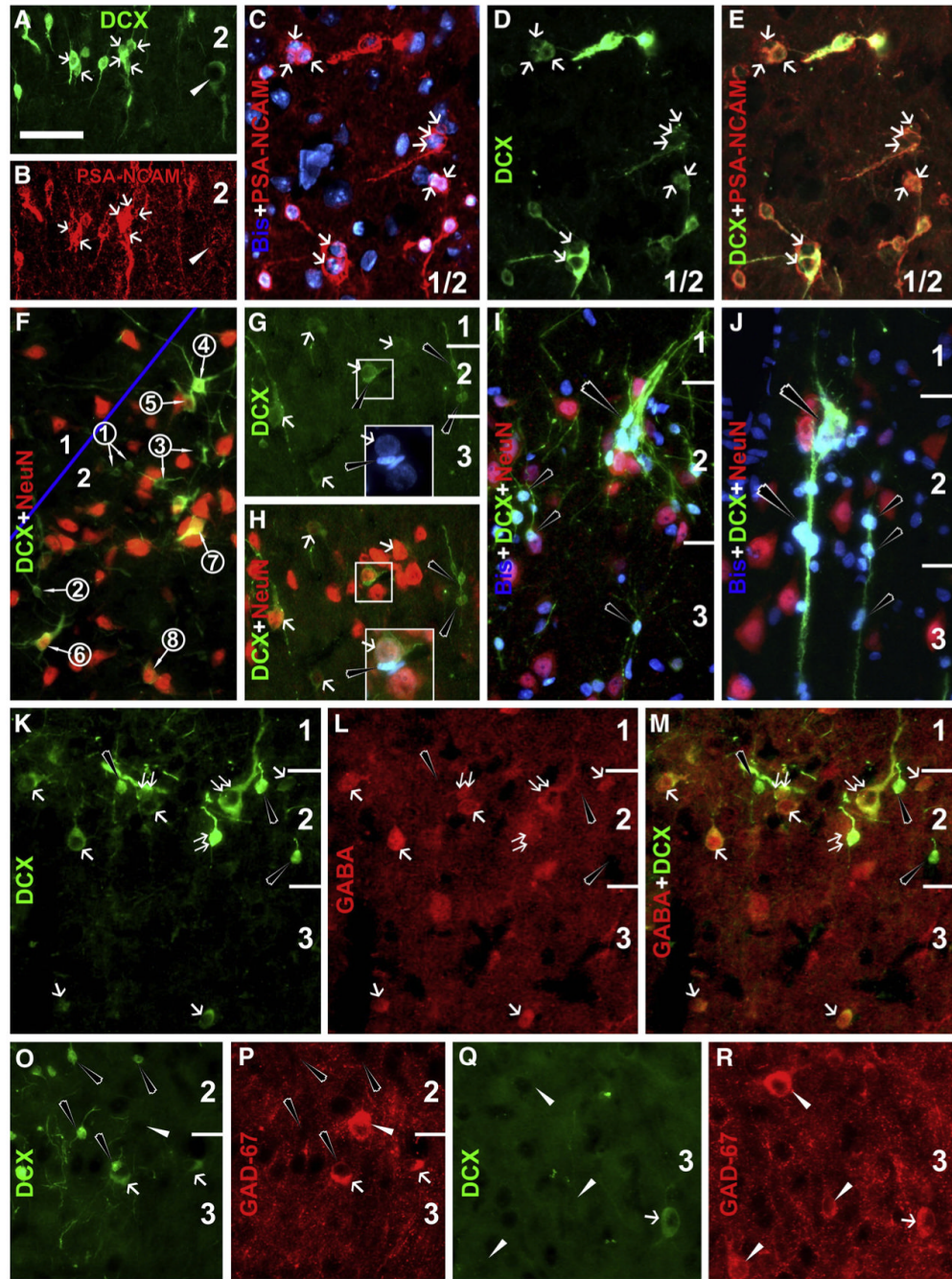


**Fig. 5.** Colocalizations of doublecortin (DCX) and polysialylated neural cell adhesion molecule (PSA-NCAM) (A–E), neuron-specific nuclear protein (NeuN) (F–J),  $\gamma$ -aminobutyric acid (GABA) (K–M) and glutamic acid decarboxylase (GAD)-67 (O–R). Bisbenzimidazole counterstain (blue) is included in some panels. Images are from the entorhinal (A, B, I, J) and temporal areas of young adult animals, including sulcal banks where the cortex is sectioned tangentially (C–E) or obliquely (F). DCX+ cells exhibit almost a complete colocalization with PSA-NCAM (A–E), although the latter labeling is faint in large cells with reduced DCX reactivity (white arrowheads, A, B). Note that labeled cells may appose to each other forming clusters (white arrows). NeuN is expressed in larger (white arrows, G, H) but not small (black arrowheads,



G–J) cells (F–J). Panel F shows changes of relative reactivities of DCX verse NeuN among a cohort of cells with varying size and neuritic complexity. DCX levels increase, peak and then decline as cells become larger with thicker dendrites, in parallel with emergence and increase of NeuN (from artificially defined stages 1 to 8). Two tightly apposed DCX+ cells (framed) in G and H exhibit dramatic difference in size and NeuN colocalization (with and without). Panels I and J show two examples of large clusters, one with cells migrating inwardly along a chain (J). GABA labeling appears absent in the small DCX+ cells (black arrowheads), but is clear in medium to large cells with distinct (double white arrows) to reduced (single white arrow) DCX levels, including those localized deeper to the cellular band in layers II/III (K–M). GAD67 labeling appears only in medium or large cells with reduced DCX levels in layers II/III (O, P) or deeper locations (Q, R). Scale bar = 50  $\mu\text{m}$  in A applying to other panels, equal to 25  $\mu\text{m}$  in the bottom boxes in G and H.

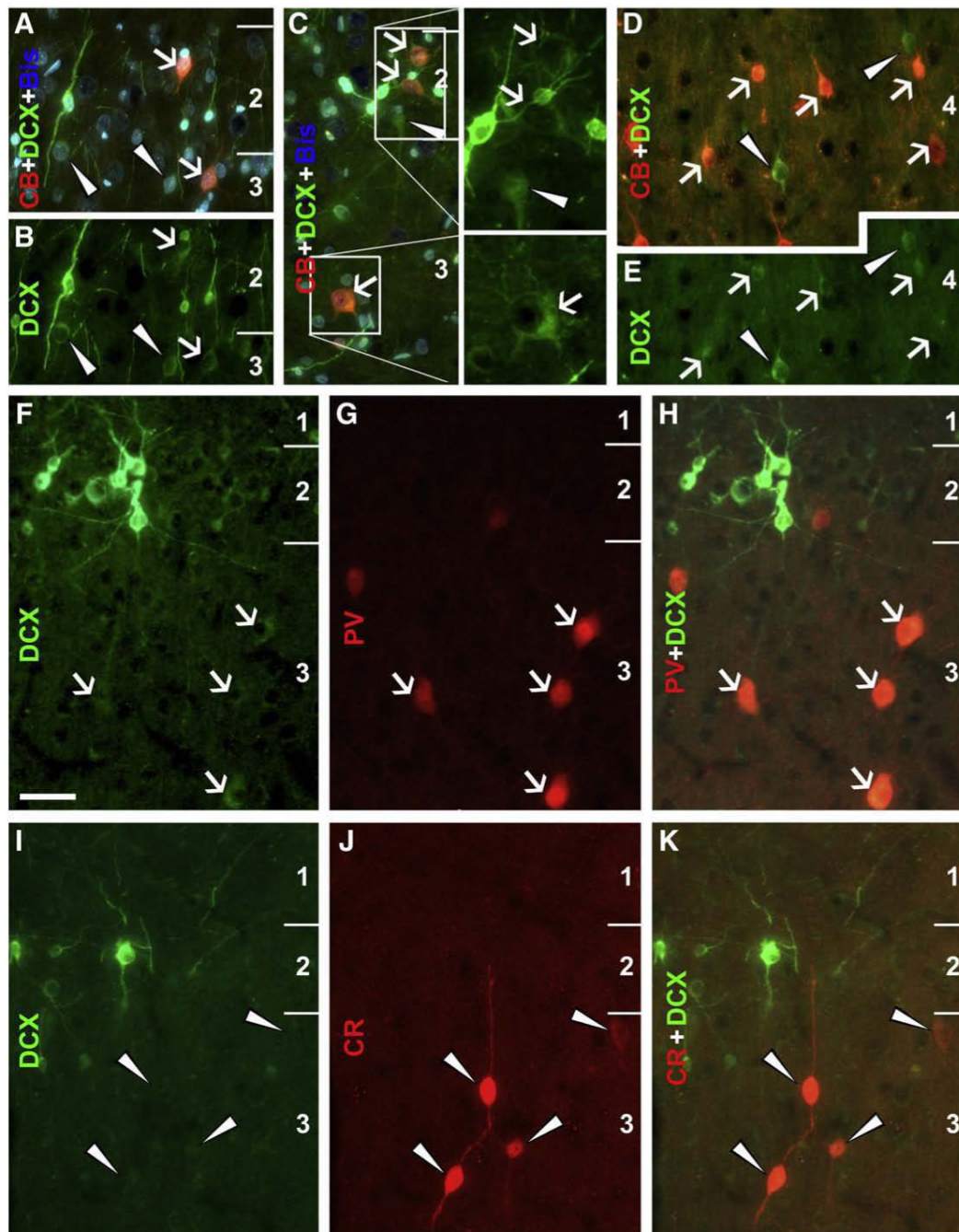


**Fig. 6.** Colocalizations of calcium-binding proteins in DCX+ cells in the temporal neocortex of an adult cat (3.5 yr-old). Panels A–C show a partial colocalization (white arrows) of calbindin (CB) in medium (A, B) to large (C, with boxed areas enlarged 2× on the right) DCX cells in layers II/III. Many medium-sized DCX+ cells in deep layers are also co-labeled for CB (white arrows, D, E), but small and some large DCX+ cells lack CB reactivity (white arrowheads, A–E). Panels F–H show parvalbumin (PV) reactivity in weakly stained DCX+ cells in layer III (white arrows). Calretinin (CR) immunoreactive neurons do not exhibit DCX labeling (I–K). Scale bar = 50 μm in F, applying to other panels.

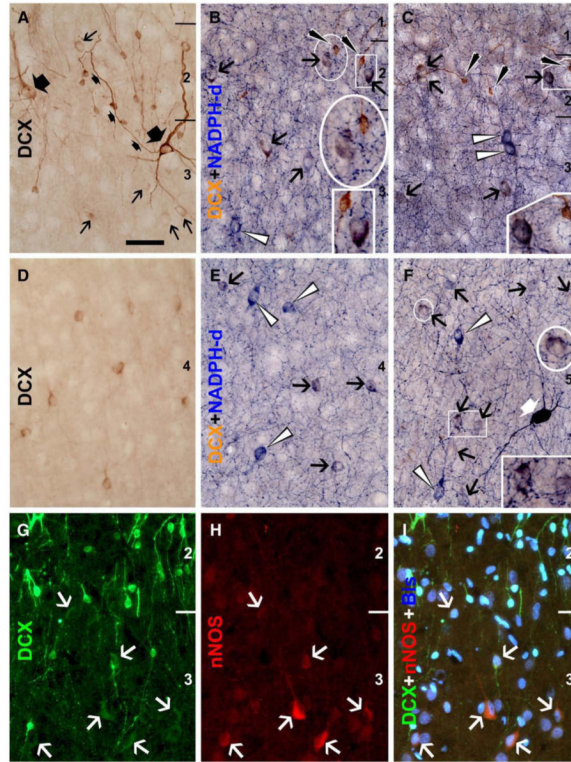


**Fig. 7.**

Colocalization of DCX with  $\beta$ -nicotinamide adenine dinucleotide phosphate diaphorase (NADPH-d) or neuronal nitric oxide synthase (nNOS) in adult cat (3.5 yr-old) cerebral cortex. Panels A–F show images from batch-processed sections with (B, C, E, F) and without (A, D) NADPH-d histochemistry (temporal cortex). Medium-sized cells (black arrows) with weak DCX reactivity in layers II/III (B, C) or IV (E, F) commonly colocalize with NADPH-d. The same situation exists for immunofluorescent colocalization of DCX and nNOS (white arrows, G–I) (entorhinal cortex). Double-labeled cells consist of a subset of type II nitrogenergic neurons, with others exhibiting stronger NADPH-d reactivity but lacking DCX (white arrowheads). Two large neurons with strong and reduced DCX reactivity are seen in panel A (marked with large fat arrows), among many small cells with varying reactivity. The axon of one large neuron is marked (small fat arrows). A type I NADPH-d neuron is seen in panel F (fat white arrow). Scale bar = 50  $\mu$ m in A, applying to other panels.

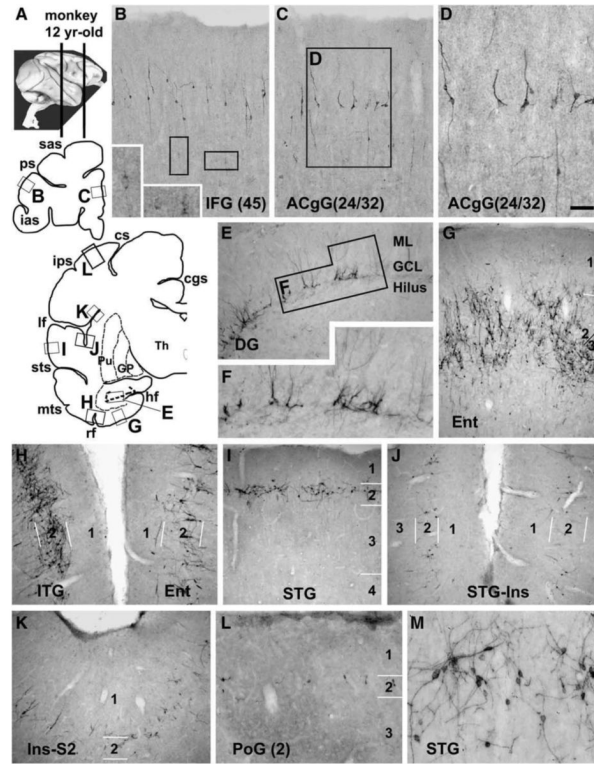


**Fig. 8.** Doublecortin immunoreactive (DCX+) cells in representative adult monkey (*Macaca mulatta*) forebrain areas, as marked on the upper-left hemispheric maps (A). Panels B–D illustrate DCX+ cells in the prefrontal areas. Distinctly and weakly stained cells are present in layers II and upper III, with some weakly stained cells also reside in deeper locations. Panels E and F show moderate labeling in dentate granular cells. Panels G–L show a ventrodorsal gradient of labeling across the hemisphere over the temporoparietal cortex. Labeled cells in the entorhinal cortex arrange according to the island formations (G). Only a few labeled cells are detected in the dorsally-located somatosensory cortex (L). At higher magnification, these cells are in bipolar or multipolar shape, with varying somal size and labeling intensity (D, M). Scale bar = 150  $\mu\text{m}$  in D applying to M, equal to 300  $\mu\text{m}$  for B, C, E, G–L and 100  $\mu\text{m}$  for M.



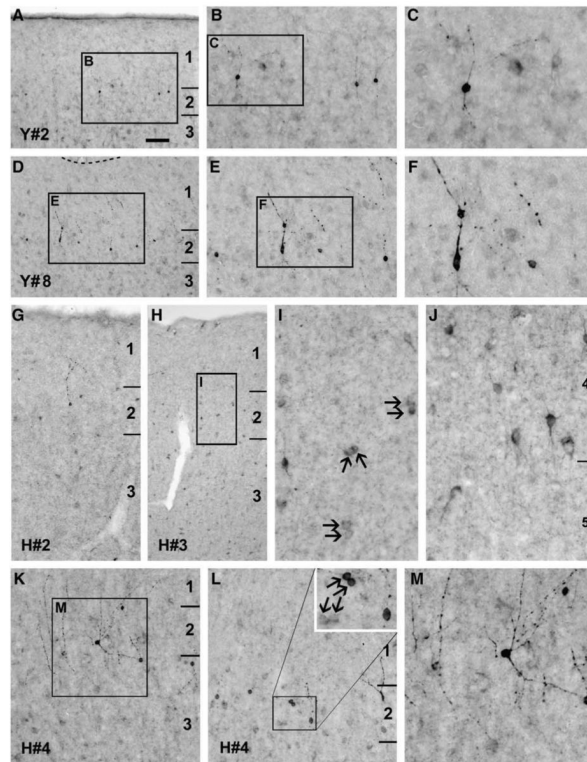


**Fig. 9.** Doublecortin immunoreactive (DCX+) cells in representative adult human temporal (A–F) and frontal (G–M) cortices prepared from surgically removed biopsies. Distinctly stained DCX+ cells exist in layer II, most of which are small bipolar (A–F) and a few multipolar (K, M). Medium-sized DCX+ cells occur across the cortex, display weak to moderate immunoreactivity, are either bipolar or multipolar, and have short processes (arrows, I). Some cells also occur in pairs (double arrows in I, L). Scale bar = 200  $\mu$ m in A applying to A, D, G, H, K, L; 100  $\mu$ m for B, E and 50  $\mu$ m for C, F, I, J, M.



**Table 1**

Patient data and cortical areas analyzed in the present study

Case#	Gender	Pathology	Age (yr)	Area studied
H#1	M	Ventricular glioma	52	SFG
H#2	F	Frontal lobe astrocytoma	36	SFG
H#3	M	Frontal lobe oligodendroglioma	44	IFG
H#4	M	Frontal meningioma	42	SFG
Y#1	M	Cavernoma	7	ITG
Y#2	F	Mesial temporal lobe sclerosis (MTS)	45	ITG
Y#3	M	Cortical dysplasia	33	ITG
Y#4	F	MTS, white matter heterotopias	38	ITG
Y#5	F	Amygdalar dysplasia	42	ITG
Y#6	F	MTS, polymicrogyria	53	ITG
Y#7	M	MTS	53	ITG
Y#8	M	MTS (post-traumatic)	38	ITG
Y#9	M	MTS	38	ITG

**Table 2**

Primary antibodies used in the present study

<b>Antibody</b>	<b>Source</b>	<b>Product code</b>	<b>Dilution</b>
Goat anti-DCX	Santa Cruz Biotech.	sc-8066	1:2000
Mouse anti-DCX	BD Biosciences	611707	1:500
Rabbit anti-DCX	Abcam	ab18723	1:500
Mouse anti-PSA-NCAM	Chemicon	MAB5324	1:2000
Mouse anti-TuJ1	Chemicon	MAB1637	1:4000
Mouse anti-NeuN	Chemicon	MAB377	1:4000
Rabbit anti-GFAP	Sigma-Aldrich	G9269	1:4000
Mouse anti-oligodendrocyte protein	Chemicon	MAB328	1:1000
Mouse anti-OX42	Bachem	T3102	1:1000
Rabbit anti-neurogranin	Chemicon	AB5620	1:2000
Mouse anti-GABA	Sigma-Aldrich	A0310	1:10,000
Mouse anti-GAD67	Chemicon	MAB5406	1:2000
Mouse anti-calbindin	Sigma-Aldrich	C9848	1:4000
Mouse anti-parvalbumin	Sigma-Aldrich	P3088	1:4000
Rabbit anti-calretinin	Sigma-Aldrich	C7479	1:2000
Rabbit anti-somatostatin	Abcam	ab22682	1:2000
Rabbit anti-nNOS	Chemicon	AB5380	1:1000